Y 3. AT 7
22/REB-32

INSTRUMENTS

UNITED STATES ATOMIC ENERGY COMMISSION

DEVELOPMENT OF PHOTOMULTIPLIER TUBES

Report No. 27 for August 1, 1957 to November 1, 1957

By
F. W. Schenkel
P. A. Snell
J. Bolakas
J. Bramley

UNIVERSITY OF ARIZONA LIBRARY
Documents Collection
MAY 25 1958

March 1958
[TISE Issuance Date]

Tube Operations Division
Allén B. DuMont Laboratories, Inc.
Passaic, New Jersey

Technical Information Service Extension, Oak Ridge, Tenn.

LEGAL NOTICE

This report was prepared as an account of Government sponsored work. Neither the United States, nor the Commission, nor any person acting on behalf of the Commission:

A. Makes any warranty or representation, express or implied, with respect to the accuracy, completeness, or usefulness of the information contained in this report, or that the use of any information, apparatus, method, or process disclosed in this report may not infringe privately owned rights; or

B. Assumes any liabilities with respect to the use of, or for damages resulting from the use of any information, apparatus, method, or process disclosed in this report.

As used in the above, "person acting on behalf of the Commission" includes any employee or contractor of the Commission to the extent that such employee or contractor prepares, handles or distributes, or provides access to, any information pursuant to his employment or contract with the Commission.

This report has been reproduced directly from the best available copy.

Printed in USA. Price 75 cents. Available from the Office of Technical Services, Department of Commerce, Washington 25, D. C.

AEC Technical Information Service Extension
Oak Ridge, Tennessee

RIB-32

REPORT #27

DEVELOPMENT OF

PHOTOMULTIPLIER TUBES

Prepared by: F. W. Schenkel
P. A. Snell
J. Bolakas
J. Bramley

Approved by: B. R. Linden
K. A. Hoagland

Contract No. AT(30-1)-1336
Atomic Energy Commission
P. O. Box 30 Ansonia Station
New York 23, New York

Period Covered By Report

August 1, 1957 to November 1, 1957

ALLEN B. DU MONT LABORATORIES, INC.
Tube Operations Division
2 Main Avenue
Passaic, New Jersey

LARGE AREA MULTIPLIER PHOTOTUBES

A. 8 Inch Flat Face Tube (K1534)

Various attempts have been made to seal an 8 inch, flat face plate to a 430 alloy metal envelope. Fig. 1 shows the envelope design which is believed to be superior to the designs illustrated in QR #26.

In attempts to make a regular glass to metal seal the face plate would become somewhat distorted and no longer maintain its flat surface. Due to the fact that the glass cannot be distorted it is necessary to utilize low temperature glasses as a sealing agent. After two sealing attempts, it was concluded that the face plate must be slightly oversized and have a 5 degree taper at the periphery to facilitate proper seating. When the face plate seal is made the metal cone will expand allowing the face plate to drop into place. Upon cooling the assembly a compression seal is obtained.

Recently a successful seal was made utilizing Corning #186 frit. This frit was applied to the rim of the face plate and partially fired. Likewise frit was applied to the rim of the metal envelope and partially fired. The face plate was then set into the metal cone and additional powdered frit was wedged between the glass and the metal. The complete unit was then placed in an oven for the required bake.

The oven was started off at room temperature and gradually increased to 430°C where it was maintained for a period of 1 hour. At the conclusion of this time the assembly was allowed to cool slowly back to room temperature.

B. 12 Inch Fused Quartz Flat Face Tube

QR #26 describes a process which can be utilized in making a hermetic seal between fused quartz and Kovar. Experimentation with this process has proven rather unsuccessful in a number of attempts that have been made in sealing small diameter fused quartz face plates to kovar cups. Various procedures are now in progress. Basically, the Telefunken process is utilized in producing these seals. This process is essentially as follows:

The fused quartz is coated with molybdenum and manganese powder. The unit is then fired in a wet hydrogen atmosphere for 15 minutes at 1200°C. A silver ring is then placed at the interface of the fused quartz face plate and the kovar cup. The unit is then brazed in a hydrogen atmosphere for 5 minutes at 900°C. An attempt was made to utilize this process, however, the final product was unsatisfactory since the silver did not wet the kovar.

Several kovar cups are now being nickel plated and then copper plated in the sealing area. This will facilitate adherence between the brasing material and the coated kovar.

TRANSIT TIME SPREAD IN LINEAR MULTIPLIER TUBES

Determinations to minimize transit time spread in Linear Multiplier Tubes have served to crystallize the reasons for the time spread, but have not been very fruitful in offering concrete solutions to the problem.

Figure "2D" represents a dynode configuration in which all the electrons leaving dynode one strike dynode two in areas where secondary emission from dynode two can reach dynode three. Electron paths "Y" and "Z" are the extremes in very slow and very fast velocity electrons. The difference in the transit time, of "Y" and "Z" electrons, is 4.3 millimicroseconds.

Two methods of experimentation were employed to study different dynode structures and potentials.

The first method incorporated the use of resistive paper on which electrodes, twenty times their actual size, were painted with a conductive silver-paint. D.C. potentials with relative magnitudes to simulate actual operating conditions, were connected to each electrode. Pencil plots of equipotential lines were obtained using a null detector and associated bridge circuit. The electron trajectories were plotted using the conventional circle or parabolic methods.

A less tedious and less time consuming method made use of the well known "rubber model". A sheet of surgical rubber,

stretched over dynode surfaces whose relative heights represent potential difference, gives a very good study of voltage gradients. Steel ball bearings, 3/16" to 1/16" in diameter, rolling from dynode one to two, closely approximate the paths of the electrons. The dynode configurations were again twenty times the size of those used in the actual multiplier structure, and elevation gradients did not exceed three inches to preserve uniform rubber stretching.

It was immediately apparent that a very poor voltage gradient exists for half of the first dynode in the proximity of the mesh. Also an extremely sharp gradient was evidenced near the first and third dynode.

Figure 2A, B, and C, shows several unsuccessful attempts at using accelerator wires to strengthen the weak gradient. Too many electrons are collected by the accelerators in order to get a reduction in transit time spread.

Figure 2E shows that modifying the shape of the second dynode and moving it in closer to the first dynode accelerates electrons from the slow areas of dynode one. At the same time many electrons strike the second dynode in an area from which secondary electrons cannot be emitted, since no accelerating potential exists for secondaries to move to the third dynode.

Figure 2F shows a configuration in which half of the first dynode is operated with a higher negative potential. Dynode 1-A electrons moved with greater velocity but dynode 1-B

distorted the trajectories sufficiently, to cause collection by the third dynode.

There are several possible solutions to the transit time problem. By creating a stronger potential gradient between dynode one and dynode two, the transit time of all electrons will be reduced. The new transit times will be the original transit times multiplied by one over the square root of the factor by which the potential gradient was increased. Consequently the new transit time difference will be the original time difference multiplied by one over the square root of the factor by which the potential gradient was increased. This stronger potential gradient can be achieved, without causing excessive leakage, by physically separating the first dynode top-shield combination and associated ceramics, from succeeding dynodes and their associated ceramics.

This method could not be proven accurately with the rubber model because large elevation gradients cause non-uniform rubber stretching with consequent erroneous voltage gradients.

A possible verification of a shorter transit time spread utilizing stronger voltage gradients between dynode one and dynode two could be seen from a different experimental set-up. Figure 3 illustrates the experiment for determining peak pulse currents in linear multiplier tubes. By raising the potential difference between dynode one-dynode two by a factor of two over the conventional voltage difference, a shorter anode pulse width was evidenced. Transit time spread is partially responsible for the output pulse width size.

An alternate method for reducing transit time spread in the first to second dynode region is to make use of a smaller first dynode. By using a smaller first dynode the front end geometry is altered so as to increase the field gradient in the first to second dynode region. To maintain good collection efficiency when using a smaller first dynode it is necessary that the primary electrons originating from the photocathode be made to focus in a smaller area on the first dynode. At present the focus point of all the photoelectrons falls midway within the top shield dome. By moving the first dynode within the top shield dome the electron cross-over can be made to fall on the surface of the first dynode.

A future experiment, utilizing a two inch image convertor, will be conducted to determine the feasibility of this arrangement. This image convertor will have a sliding dome which can be moved between the photocathode and first dynode multiplier section of the tube. Both the multiplier section and the dome will be covered with a P1 phosphor to enable one to determine the exact dimensions and cross-over point of the electron beam emanating from the photocathode. More detailed information will be available at the conclusion of the next quarter.

PEAK PULSE CURRENTS IN LINEAR MULTIPLIER TUBES

With the circuit configuration shown in Figure 3, an experiment was performed to determine the peak pulse anode current that can be drawn for selected interstage voltages.

Data was obtained which permitted a graphical plot to be made of output anode current versus electron-gun beam current. Measurements of the electron flow reaching the first dynode could not be made with any reasonable accuracy, therefore the assumption was made that the number of electrons striking the first dynode are linearly proportional to the electron-gun beam current.

Three sets of graphs, Figure 4, were obtained, each with a different interstage voltage. The voltages chosen were 105, 150, and 210 volts per stage.

Reference to the graphs, in Figure 4, indicates an almost linear response for the lower anode currents, and a saturation response for the higher anode currents.

For 210 volts per stage, the maximum current drawn is 0.48 amperes, while the linear response ranged between zero and 0.37 amperes. For 150 volts per stage, the maximum current drawn is 0.27 amperes, while the linear response ranged between zero and 0.175 amperes. For 105 volts per stage, the maximum current drawn is 0.14 amperes, while the linear response ranged between zero and 0.115 amperes.

Apparently, to obtain ultimate saturation, Figure 4, a beam-current larger than was available, (320 microamperes), is necessary. Future experiments will incorporate a tube capable of delivering an electron beam of higher intensity.

Accelerator wires, between dynodes 6 and 7, 7 and 8, and 8 and 9, serve to increase the output current when they are connected to the potentials of dynode 7, dynode 9, and the anode respectively.

The observed output pulse widths were slightly larger for the larger anode currents. The range of widths was from 70 to 110 millimicroseconds.

The circuitry coupling the anode of the multiplier structure to the measuring equipment was not designed for a wide band width and high frequency response since pulse amplitude and not pulse width was of prime interest. This fact was probably responsible for the large output pulse widths read on the oscilloscope. The input pulse width to dynode one ranged from 15 to 20 millimicroseconds, at an aperture sweep rate of 100,000 p.p.s. The sweep voltage required to produce the input pulse was obtained directly from square wave rate generator of the "517 Tektronix" oscilloscope. In future experiments the input pulse will be much shorter. The pulse will be obtained from the "Du Mont 404" pulse generator, and it will exhibit from 1/2 to 1/3 the rise time of the pulse given by the Tektronix oscilloscope. The size of the aperture preceding dynode one is another factor which determines the input pulse width to dynode one. A new tube is under construction and it will incorporate a smaller aperture in order to decrease the pulse width to dynode one.

The output current from the anode was measured by means of a 236 ohm load resistance from anode to ground. The oscilloscope with its 170 ohm impedance, when placed across this load resistance effectively causes the output pulse to be developed across a 99 ohm load.

A reasonable assumption is made that any capacity effects of the load resistor are not sufficient to cause an a.c. bypass of the pulse to ground, and thereby negating the effect of the 236 ohm resistance.

The three experimental runs illustrated by Figure 4, were performed in two slightly different manners. Throughout one run the electron beam emanating from the electron-gun was sharply focused, as contrasted to holding the electron beam size constant throughout the other run. The sharply defined beam was very selective indicating the first dynode had non-uniform sensitivity.

The resultant anode pulse was slightly stronger for the sharpened beam, and the electron trace on the oscilloscope was sharper and therefore could be more accurately read. A discrepancy of 15% to 20% in collected anode current has been found in comparing the two methods. Where the two sets of curves coincide, the beam-current is too strong to be sharply focused, and therefore is in all probability causing a decrease in output current.

An experiment was devised in an attempt to determine which dynode in the multiplier structure causes the saturation effects evident in the anode output current curves. Curves of current impinging upon the last seven dynodes versus beam current indicated that all these seven dynodes were saturating. It was pointed out that an erroneous assumption may have been the cause of the seven similarly shaped curves. The experiment will be performed again but with the corrected approach.

A "Tektronix 517" oscilloscope was used in making all current measurements. The last seven dynodes had calibrated load resistors in their associated circuitry to facilitate use of the oscilloscope. The flow of electrons either leaving or entering the dynodes can be detected by the potential developed across each resistor. To isolate the oscilloscope from the high d.c. voltage a .02 micro-farad condenser is used. This condenser neither distorts or attenuates the output pulse.

The electron flow associated with dynodes one, two and three is extremely small. Consequently the voltages developed across calibrated load resistors in these dynode circuits are much too weak to be detected by the oscilloscope. A five stage transistorized pre-amplifier, on loan from the Atomic Energy Commission, is to be used to amplify the weak signals sufficiently to be read on the oscilloscope. Preliminary tests indicate the frequency response of the amplifier is adequate to supply amplification without distortion.

The revised experiment will be conducted to determine:

(1) The percentage of current intercepted by the anode which is in the direct path of electrons travelling between the last and next to last dynode.

(2) The maximum peak pulse current that can be drawn using the new experimental tube which will emit a higher beam current and consist of an electron multiplier structure utilizing 12 dynodes.

(3) Space charge saturation in the last six stages of the multiplier structure which can be determined by plotting the sixth dynode current (as an independent variable) vs. the collected currents in the succeeding stages.

REGENERATION IN MULTIPLIER PHOTOTUBES

When operating a multiplier phototube with high signal currents it has been found that blue light is generated within the tube. This light is found to originate mainly at these points where the current density is known to be high. This light is probably produced mainly by the ionization of cesium atoms within. In order to avoid having this light cause regeneration in the photocathode, multiplier phototubes are being constructed using special envelopes. Several such tubes are under construction using a metal envelope. Another group of tubes are being built using a metal ring light trap. These tube types will be ready for evacuation within the next several weeks at which time more conclusive information can be made available.

DEVELOPMENT OF PHOTOCATHODE SURFACES

Effort has been expended in the development of a photocathode surface which is sensitive in the ultraviolet portion of the spectrum and has little or no sensitivity to visible light. Experimental multiplier phototubes were constructed employing a cesium telluride photosensitive surface. Preliminary tests have shown that this surface has practically no white light sensitivity but exhibits very high response in the ultraviolet. Apparently the ultraviolet response is equal to that obtained with a cesium antimony photosurface used in conjunction with a fused silica window. A spectral response characteristic will be obtained in the near future using a monochromator. It is expected that more conclusive data will be available at the close of the next quarterly period at which time these tubes will have undergone more complete electrical testing.

DEVELOPMENT OF IMPROVED ELECTRON OPTICS FOR THE 16 INCH MULTIPLIER PHOTOTUBE

In order to derive a more efficient electrostatic optical system to be used in conjunction with a large area, 16 inch diameter multiplier phototube the following analysis has been made. This analysis is based on a similar optical system which is to be used in the design of a 16 inch diameter image convertor.

At the end of the work on the minifier, we reached the conclusion that the relaxation method constituted the best approach to the solution of the boundary value potential problem inside an axisymmetrical image convertor. In this method, the potential is determined not at every point in an axial plane, as is accomplished by an analytical method, but over a mesh system. Thus Laplace's differential equation

$$\frac{\partial^2 V}{\partial r^2} + \frac{1}{r}\frac{\partial V}{\partial r} + \frac{\partial^2 V}{\partial z^2} = 0 \qquad (1)$$

which holds in continuous space, is replaced by a difference equation, which determines the potential at a point in terms of the potentials at neighboring points. We shall label the points by the numbers 0, 1, 2, 3, and 4 and denote by $S_1 a$ the distance from the point 0 to the point 1, by $S_2 a$ the distance from 0 to 2, etc., and by Ia the distance from 0 to the axis. (See Fig. 5.) This notation conforms to that used in Durand's textbook.[1] The difference equation, which gives V_0 in terms of V_1, V_2, V_3, and V_4 is:

$$\left[\frac{2I}{S_1 S_3} + \frac{2I + (S_4 - S_2)}{S_2 S_4}\right] V_0 = \frac{2I}{S_1(S_1+S_3)} V_1 + \frac{2I}{S_3(S_1+S_3)} V_3 + \frac{2I+S_4}{S_2(S_2+S_4)} V_2 + \frac{2I-S_2}{S_4(S_2+S_4)} V_4 \qquad (2)$$

As a matter of convenience, we choose a mesh, which is uniform throughout the interior, i.e. one for which $S_1 = S_2 = S_3 = S_4$ with the resulting simplification of the difference equation to

$$4V_0 = V_1 + V_3 + \left(1 + \frac{1}{2I}\right) V_2 + \left(1 - \frac{1}{2I}\right) V_4 \qquad (3)$$

The simplifying condition will, as a rule, not hold in the vicinity of the boundary where the potential must be determined by means of Eq. (2). For a point on the axis V_0 is determined in terms of only three neighboring potentials, V_1, V_2, and V_3 by the difference equation

$$\left[\frac{2}{S_1^2} + \frac{1}{S_1 S_3}\right] V_0 = \frac{V_1}{S_1(S_1+S_3)} + \frac{V_3}{S_3(S_1+S_3)} + \frac{2V_2}{S_1^2} \qquad (4)$$

which for an interior point simplifies to

$$6V_0 = V_1 + 4V_2 + V_3 \qquad (5)$$

Eqs. (2) and (4) correspond to Durand's Eqs. (74) and (75) on p. 463, in which the errors have been corrected.

In the relaxation method, the zeroth order approximation consists merely of a guess as to the potential values at all mesh points when the values are known over the boundary. This guess is improved at the next, i.e. first order, approximation by the application at each point of the appropriate difference equation. (One of the Eqs. (2), (3), (4), or (5), depending on the location of the point.) When one order of approximation, or relaxation step, has been completed for all mesh points, the process is repeated.

There are two main drawbacks to this method if it is applied injudiciously. The first is the large number of points at which the potential has to be computed to insure a high degree of accuracy in the solution. The second is the slowness of convergence of the relaxation, i.e. iteration, process if the original guess was not good enough. While methods to

improve convergence are known[2], we found that they are inapplicable in cases, such as the present, where there are sharp variations in potential along the boundary. We also found, however, that a high degree of accuracy could be obtained without excessive labor by following the following procedures:

The potential is first determined, over a coarse mesh, i.e. at relatively few points. If after the first two or three relaxation steps, a definite trend is noticed in the potential values, a suitable adjustment is made. For example if the potential values in a certain region keep increasing appreciably at each relaxation step, they are raised by an intuitive guess before proceeding to the next relaxation step. The process is continued in a given region (which must include an appreciable portion of the entire domain) until the condition given below is found to hold at every point of the region. This condition may be put in the form

$$(V^A - V^B)/V^B < p, \qquad (6)$$

where V^A and V^B are the values obtained at some point at the last two relaxation steps and p is an arbirarily preassigned value.

At this stage a finer mesh is introduced, each cell of the new mesh being 1/4 the size of the original one. The potential at the center of each coarse mesh is calculated by means of the relation

$$4V_0 = \left(1+\frac{1}{2I}\right)(V_5 + V_6) + \left(1-\frac{1}{2I}\right)(V_7 + V_8) \qquad (7)$$

the notation being shown in Fig. 6. The other points of the fine mesh are determined by means of Eqs. (3) or (5) depending on their location with respect to the axis. After this usually only one or two relaxation steps are needed for the entire fine mesh domain to obtain the potential to a high degree of accuracy. We believe that our results are accurate to about 0.1% for a very large portion of the domain and to better than 1% for the rest. We believe that this high accuracy is due both to the technique described and to a good zeroth order approximation.

To permit better visualization of the potential distribution inside the tube, we plotted equipotential lines at fixed potential values. As a matter of convenience, we assumed the potential to be V = 0 at the cathode and V = 100 at the anode, with the other electrodes being at intermediate values. The equipotential lines were plotted for V = 10, 20, etc., with intervening lines in regions of special interest. To find the location of the points corresponding to specified potential values, interpolation was used. It was possible to tell by inspection of the rate of variation of potential in a certain region whether quadratic interpolation was necessary or whether linear interpolation would be sufficient.

An example of the application of the method to the design of multiplier phototubes is shown in Fig. 7, which represents the equipotential map at the front end of a 15" multiplier phototube.

Once the equipotential lines are known, the electron path can be obtained graphically. This subject is discussed in great detail in the literature.[3] We tried to follow the standard procedure but found that the error introduced at each step could be sufficiently high to invalidate the final result since for the long tube under consideration the construction must be repeated some 15 times. Zworykin mentions an accurate though extremely laborious method for finding the electron trajectory numerically. (See Section 3.4 of ref. 3.) We believe that a technique more easily adapted to computation with a large scale digital computer can be developed. This work will be carried out during the next contract period.

REFERENCES

1
Durand, E., ELECTROSTATIQUE ET MAGNETOSTATIQUE, Masson et Cie, 1953, p. 461 - 463.

2
Shortley, G.; Weller, R.; Darby, P; & Gamble, E. H., Numerical Solution of Axisymmetrical Problems, with Applications to the Electrostatics & Torsion, JOURNAL OF APPLIED PHYSICS, Vol. 18-1/47, p. 116 - 129.

3
Zworykin, J. K. & Morton, G. A., Television 2nd Ed. 1954, John Wiley Sons, Inc., Sect. 3.5, p. 104ff.

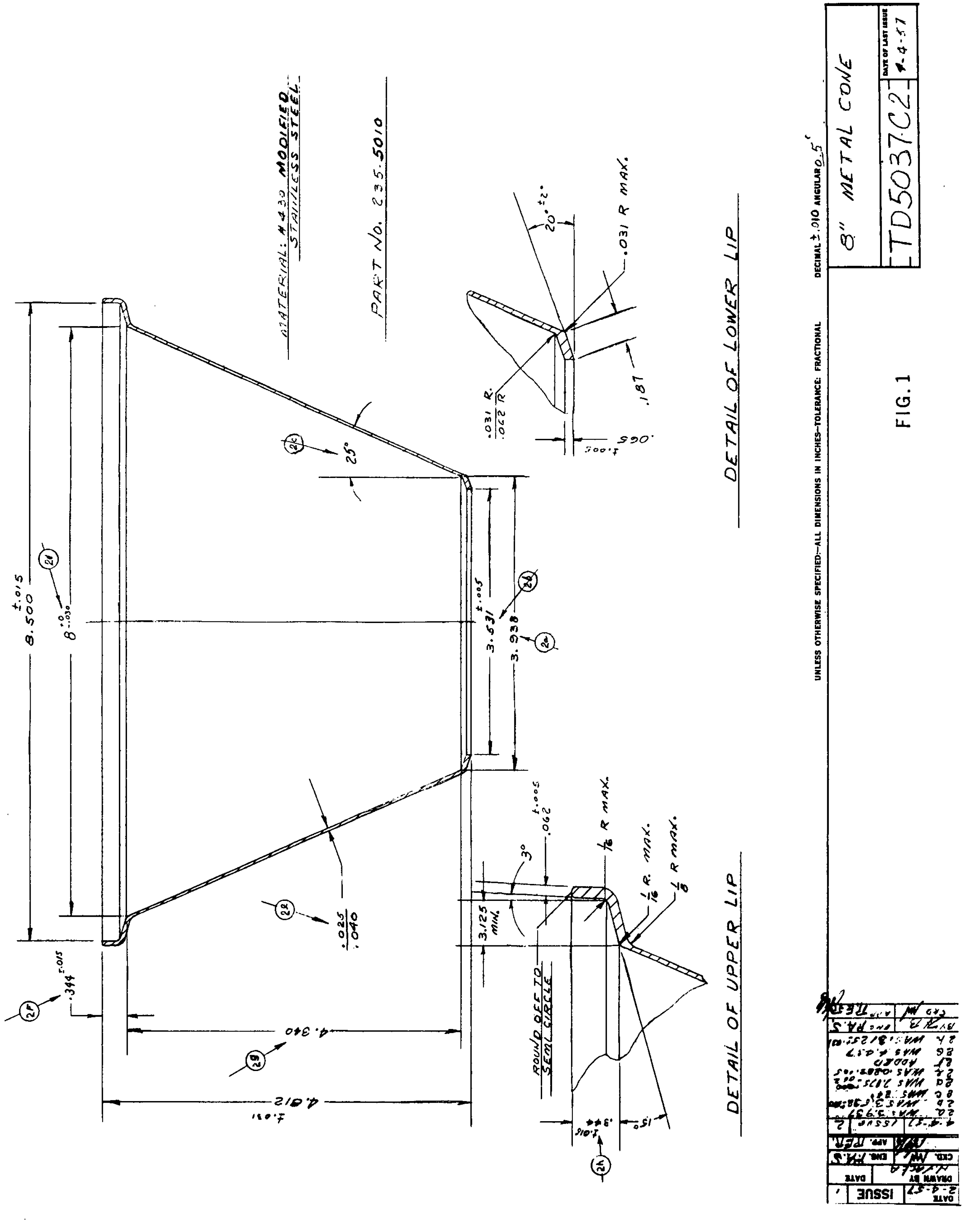
MATERIAL: #430 MODIFIED STAINLESS STEEL
PART No. 235-5010
DETAIL OF LOWER LIP
DETAIL OF UPPER LIP
ROUND OFF TO SEMI CIRCLE
.031 R MAX.
20° ±2°
.187
.065 ±.005
.031 R
.062 R
25°
3.531 ±.005
3.938
8.500 ±.015
8 +.0 -.030
.025
.040
.344 ±.015
4.340
4.812 ±.031
3.125 MIN.
3°
.062 ±.005
1/16 R MAX.
1/16 R. MAX.
1/8 R MAX.
.15°
UNLESS OTHERWISE SPECIFIED—ALL DIMENSIONS IN INCHES—TOLERANCE: FRACTIONAL
DECIMAL ±.010 ANGULAR 0.5°
8" METAL CONE
TD5037C2
DATE OF LAST ISSUE
4-4-57
ISSUE
DATE
2-4-57
DRAWN BY
CKD.
ENG.
APP.

FIG.1

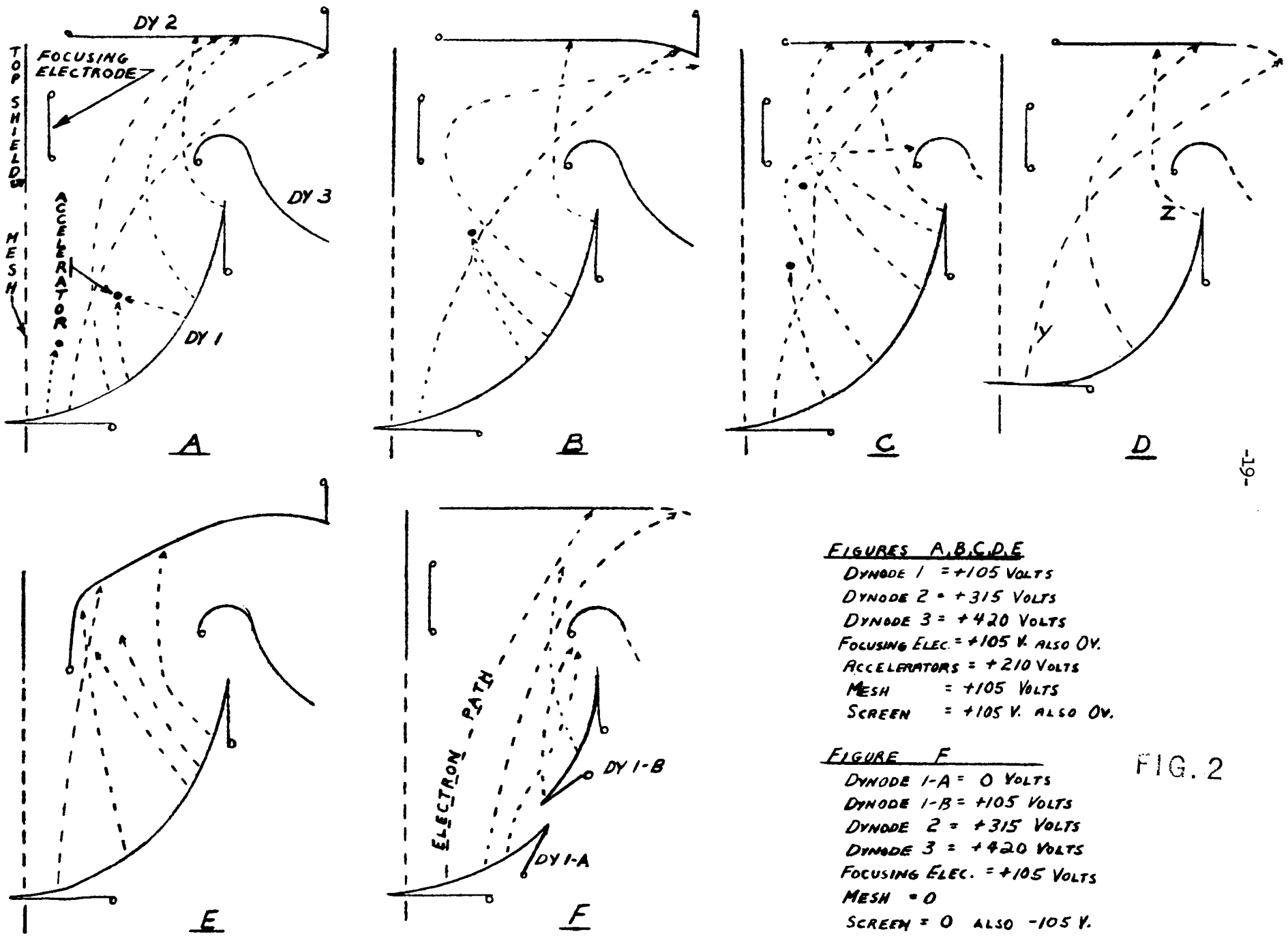

FIGURES A,B,C,D,E

DYNODE 1 = +105 VOLTS
DYNODE 2 = +315 VOLTS
DYNODE 3 = +420 VOLTS
FOCUSING ELEC. = +105 V. ALSO 0V.
ACCELERATORS = +210 VOLTS
MESH = +105 VOLTS
SCREEN = +105 V. ALSO 0V.

FIGURE F

DYNODE 1-A = 0 VOLTS
DYNODE 1-B = +105 VOLTS
DYNODE 2 = +315 VOLTS
DYNODE 3 = +420 VOLTS
FOCUSING ELEC. = +105 VOLTS
MESH = 0
SCREEN = 0 ALSO -105 V.

FIG. 2

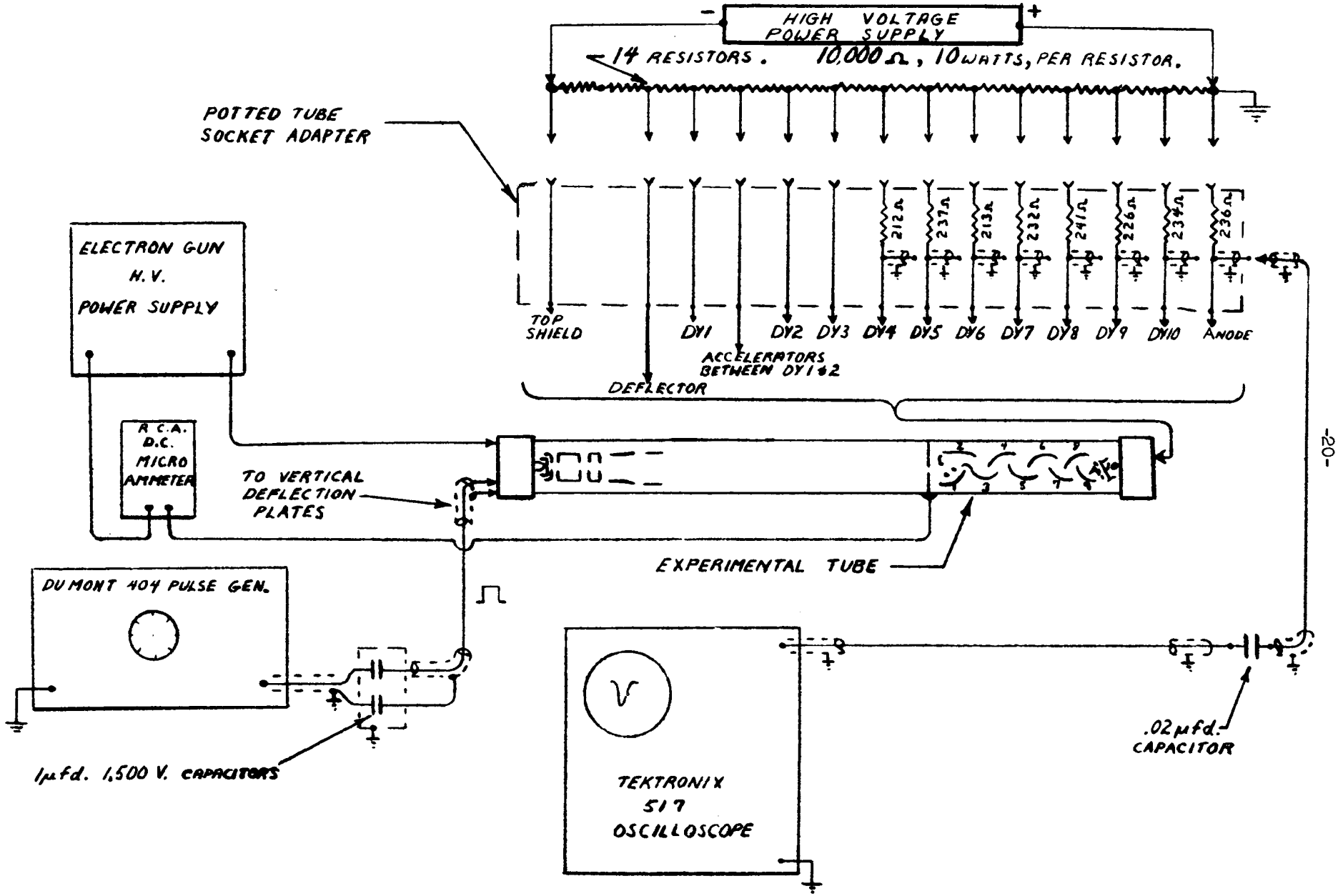
HIGH VOLTAGE POWER SUPPLY
14 RESISTORS. 10,000 Ω, 10 WATTS, PER RESISTOR.
POTTED TUBE SOCKET ADAPTER
ELECTRON GUN H.V. POWER SUPPLY
212Ω
237Ω
213Ω
232Ω
241Ω
226Ω
234Ω
236Ω
TOP SHIELD
DY1
DY2
DY3
DY4
DY5
DY6
DY7
DY8
DY9
DY10
ANODE
ACCELERATORS BETWEEN DY1&2
DEFLECTOR
R.C.A. D.C. MICRO AMMETER
TO VERTICAL DEFLECTION PLATES
EXPERIMENTAL TUBE
DUMONT 404 PULSE GEN.
V
TEKTRONIX 517 OSCILLOSCOPE
.02 μfd. CAPACITOR
1 μfd. 1,500 V. CAPACITORS

FIG. 3

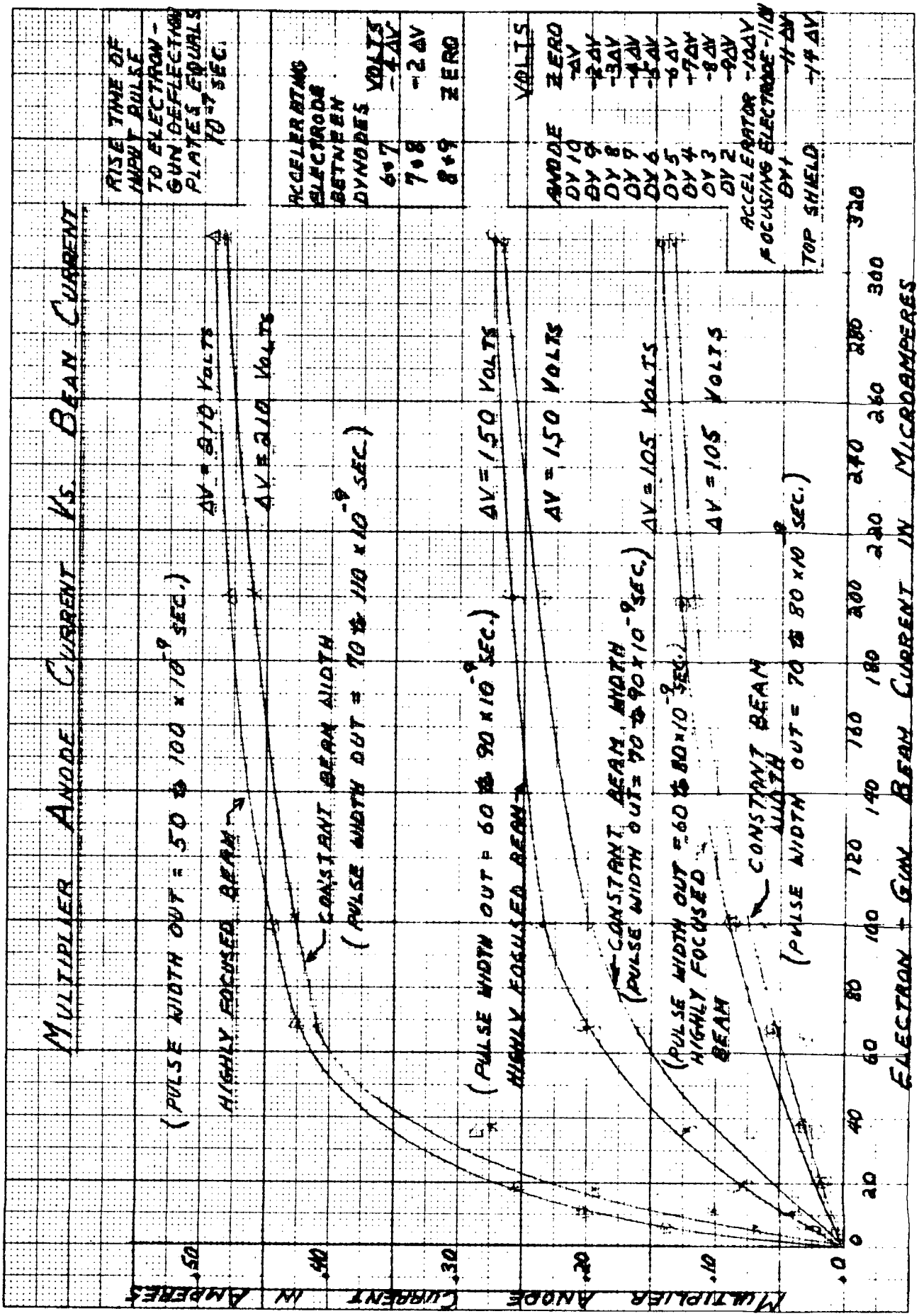
Multiplier Anode Current Vs. Beam Current
(Pulse width out = 50 to 100 x 10⁻⁹ sec.)
ΔV = 270 Volts
ΔV = 210 Volts
Highly focused beam
Constant beam width
(Pulse width out = 70 to 110 x 10⁻⁹ sec.)
(Pulse width out = 60 to 90 x 10⁻⁹ sec.)
ΔV = 150 Volts
Highly focused beam
Constant beam width
(Pulse width out = 70 to 90 x 10⁻⁹ sec.)
ΔV = 105 Volts
(Pulse width out = 60 to 80 x 10⁻⁹ sec.)
Highly focused beam
Constant beam width
(Pulse width out = 70 to 80 x 10⁻⁹ sec.)
ΔV = 105 Volts
Rise time of input pulse to electron-gun deflection plates equals 10⁻⁷ sec.
Accelerating electrode between dynodes 6 & 7 Volts −4ΔV
7 & 8 −2ΔV
8 & 9 Zero
Volts
Anode Zero
Dy 10 −ΔV
Dy 9 −2ΔV
Dy 8 −3ΔV
Dy 7 −4ΔV
Dy 6 −5ΔV
Dy 5 −6ΔV
Dy 4 −7ΔV
Dy 3 −8ΔV
Dy 2 −9ΔV
Accelerator −10ΔV
Focusing electrode −11ΔV
Dy 1 −11ΔV
Top shield −11ΔV
Multiplier Anode Current in Amperes
Electron Gun Beam Current in Microamperes
0
10
20
30
40
50
0
20
40
60
80
100
120
140
160
180
200
220
240
260
280
300
320

FIG. 4

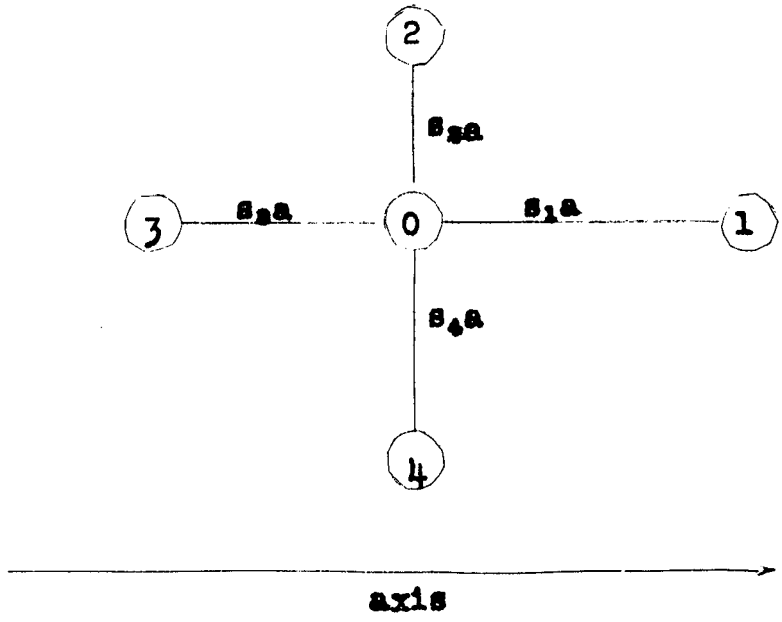
2
s_2a
3
s_3a
0
s_1a
1
s_4a
4
axis

Fig. 5

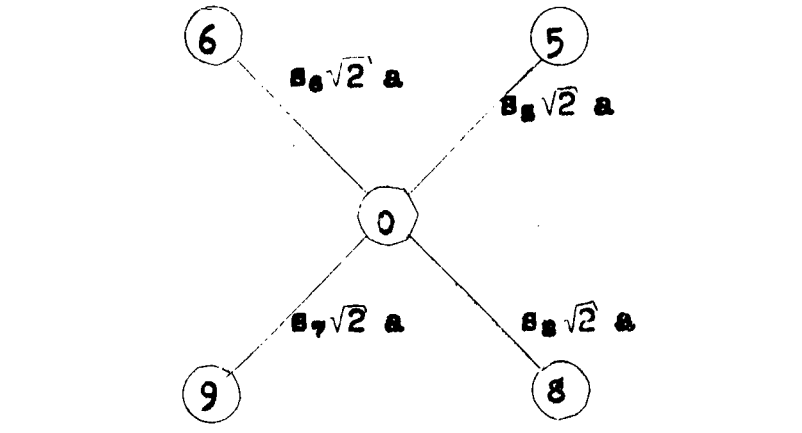
6
$s_6\sqrt{2}\,a$
5
$s_5\sqrt{2}\,a$
0
$s_7\sqrt{2}\,a$
$s_8\sqrt{2}\,a$
9
8
axis

Fig. 6

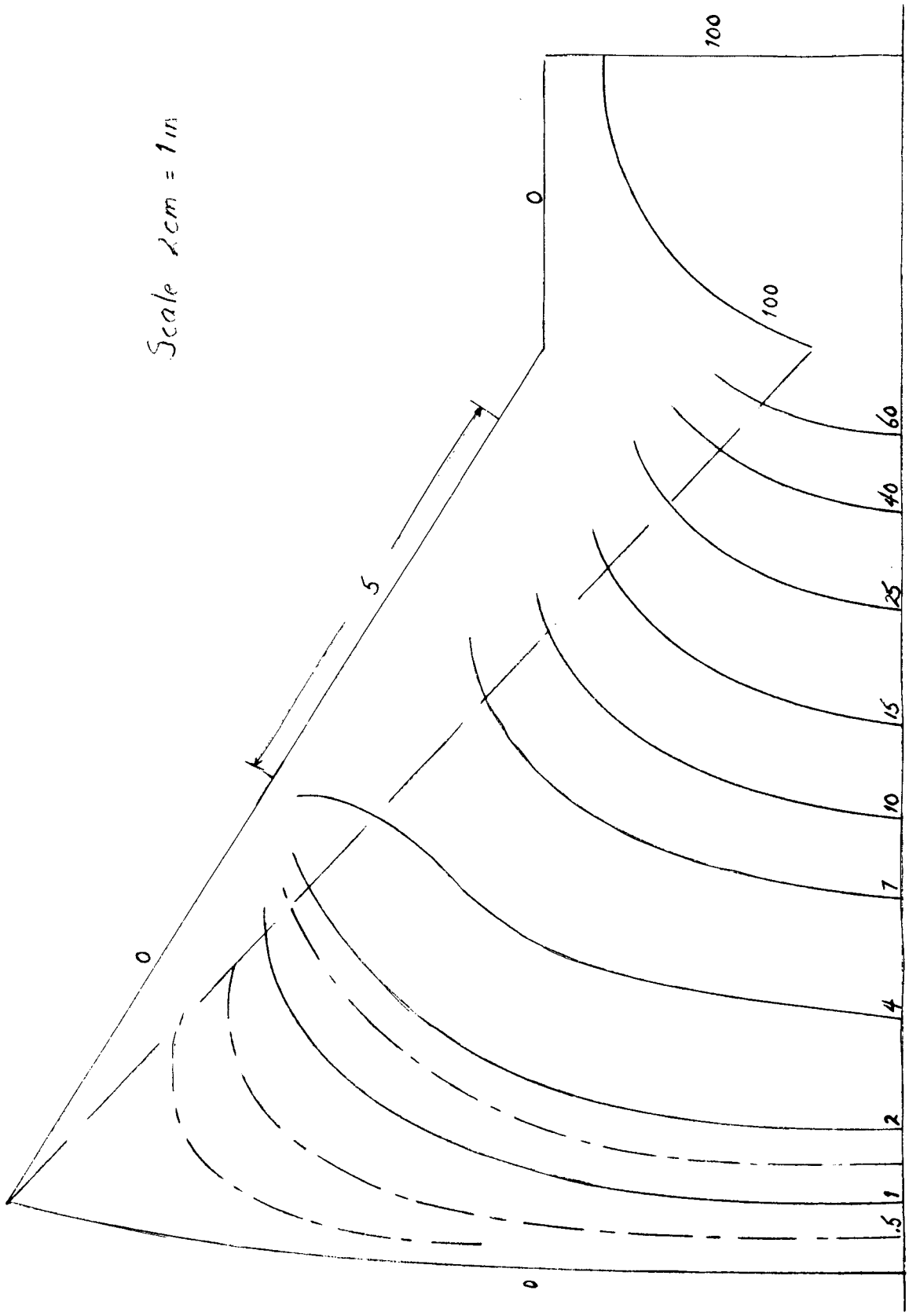

Figure 7